How Can Tropical Pacific Ocean Heat Transport Vary?

WILCO HAZELEGER

Royal Netherlands Meteorological Institute (KNMI), De Bilt, Netherlands

RICHARD SEAGER, MARK A. CANE, AND NAOMI H. NAIK

Lamont-Doherty Earth Observatory, Columbia University, Palisades, New York

(Manuscript received 26 August 2002, in final form 22 May 2003)

ABSTRACT

Pacific Ocean oceanic heat transport is studied in an ocean model coupled to an atmospheric mixed-layer model. The shallow meridional overturning circulation cells in the Tropics and subtropics transport heat away from the equator. The heat transport by the horizontal gyre circulation in the Tropics is smaller and directed toward the equator. The response of the Pacific oceanic heat transport to El Niño–like winds, extratropical winds, and variations in the Indonesian Throughflow is studied. Large, opposing changes are found in the heat transport by the meridional overturning and the horizontal gyres in response to El Niño–like winds. Consequently, the change in total heat transport is relatively small. The overturning transport decreases and the gyres spin down when the winds decrease in the Tropics. This compensation breaks down when the Indonesian Throughflow is allowed to vary in the model. A reduced Indonesian Throughflow, as observed during El Niño–like conditions, causes a large reduction of poleward heat transport in the South Pacific and affects the ocean heat transport in the southern tropical Pacific. Extratropical atmospheric anomalies can affect tropical ocean heat transport as the tropical thermocline is ventilated from the extratropics. The authors find that changes in the heat loss in the midlatitudes affect tropical ocean heat transport by driving an enhanced buoyancy-driven overturning that reaches into the Tropics. The results are related to observed changes in the overturning circulation in the Pacific in the 1990s, sea surface temperarture changes, and changes in atmospheric circulation. The results imply that the ratio of heat transport in the ocean to that in the atmosphere can change.

1. Introduction

The excess of net incoming radiation at the top of the atmosphere in the Tropics and the deficit of net radiation in the extratropics requires poleward energy transport in the atmosphere and oceans to mediate the radiative imbalance. Recent estimates, based on satellite-derived top of the atmosphere radiation and atmospheric reanalysis data, show that the ocean dominates the energy transport in the Tropics (Trenberth and Caron 2001). Here we will focus on the part of the ocean heat transport that occurs in the tropical Pacific Ocean. In the Pacific the ocean heat transport peaks at 0.96 PW at 15°N. In the South Pacific poleward heat transport peaks at 0.92 PW at 10°S according to Trenberth and Caron (2001). Deep hydrographic data at low latitudes are sparse. But in combination with inverse models, ocean data also indicates a relatively strong ocean heat transport at low latitudes (Ganachaud and Wunsch 2000, 2003). Ocean heat transport estimates derived from surface flux climatologies show maxima in the Tropics, but with amplitudes almost a factor of 2 smaller than estimates from atmospheric reanalysis data.

Although meridional heat transport is one of the most fundamental properties of the climate system, the error bars on all estimates of mean ocean heat transports are large. This may explain why temporal variability in heat transport in the coupled climate system has hardly been addressed, except for seasonal variations (e.g., Bryan 1982; Jayne and Marotzke 2001). However, climate in the tropical Pacific has undergone large variations at low frequencies (Guilderson and Schrag 1998; Zhang et al. 1997) and might also change in the near future (Timmermann et al. 1999). It is not known how the atmosphere and ocean heat transports are involved in these climate changes.

In the Pacific, wind-driven subtropical cells transfer mass from the equator poleward and compensating equatorward transport occurs in the interior (McCreary and Lu 1994; Liu 1994). It has been suggested that changes in the strength of these cells induce changes in meridional ocean heat transport and forces low frequency variability in the equatorial Pacific. McPhaden and Zhang (2002) showed that the volume transport by

Corresponding author address: W. Hazeleger, Royal Netherlands Meteorological Institute (KNMI), P.O. Box 201, 3730 AE, De Bilt, Netherlands.
E-mail: hazelege@knmi.nl

the meridional overturning in the Pacific reduced in the 1990s. This would induce a reduction of the poleward meridional heat transport away from the equator and cause warming of equatorial sea surface temperatures in the 1990s. In support Nonaka et al. (2002) used model experiments to show that off-equatorial trade winds drive changes in the strength of the subtropical cells that cause decadal variations in equatorial SST. In contrast, transport of thermal anomalies by the subtropical cells are not a likely mechanism for decadal variations in the Tropics (Schneider et al. 1999; Hazeleger et al. 2001b).

If these studies are correct and ocean heat transport has decreased, then the question arises: what happened to the atmosphere heat transport? According to the ideas of Bjerknes (1964) it should have increased. His argument, which was formulated for midlatitudes, was based on the assumption that the top of the atmosphere radiation balance is hard to change and that, consequently, the total atmosphere plus ocean heat transport is invariant and its components must vary in opposition to each other. This idea gets some support because this does happen in the Tropics in climate model experiments where the specified ocean heat transport is varied (Covey and Thompson 1988; Cohen-Solal and Le Treut 1997; Clement and Seager 1999).

In stark contrast Held (2001) argues that it is the partitioning of the atmosphere and ocean heat transport that is invariant. His argument is based on the assumptions that the Hadley cell accounts for the atmosphere heat transport and that the wind-driven mean meridional overturning accounts for the ocean heat transport. Since the mass overturnings of these two cells are equal, being constrained by the same momentum flux at the air–sea interface and since the low level air temperature and specific humidity closely follow the SST, a variation in the heat transport of one has to be associated with a same sign and proportional variation in the heat transport of the other. Consequently, if McPhaden and Zhang (2002) are right and the poleward ocean heat transport declined in the 1990s, then the atmosphere heat transport from the equator to the subtropics would have had to decrease too. The top of the atmosphere radiation balance would have had to change to ensure balance. This idea gets some support from recent analyses of satellite data that show the net radiation at the top of the tropical atmosphere has changed over this time (Wielicki et al. 2002). However, differences in the domain and time periods considered make it hard to check the consistency between the satellite and ocean data.

The studies of McPhaden and Zhang (2002), Nonaka et al. (2002), and Held (2001) do not consider the transport of heat by the horizontal equatorial wind-driven gyres. However, it is well known that these move large amounts of heat *toward* the equator (e.g., Gordon et al. 2000). If the Hadley cell changes in strength, we would also expect the gyre heat transport to change. Further, large amounts of warm water are exported from the tropical Pacific into the Indian Ocean through the Indonesian Throughflow (ITF) with a compensating inflow of cooler water into the South Pacific. Changes in surface winds will also be expected to change the strength of the throughflow, as happens during the ENSO cycle (Meyers 1996; Vranes et al. 2002). In addition, the Tropics are not isolated, and it is possible that wind variations in the extratropics have a remote impact in the Tropics (e.g., Hazeleger et al. 2001a).

In the present exploratory study we will examine how tropical Pacific oceanic heat transport can vary. We will focus on the roles of the overturning cells, the transport by the horizontal wind-driven gyres, the import and export of heat by the ITF, and the exchange of heat with the midlatitudes. All of these processes have a potentially large effect on tropical SST and heat transports. We will apply atmospheric circulation anomalies in an ocean general circulation model coupled to an atmospheric mixed-layer model and analyse the changes in ocean heat transport. Since we are interested in low frequency changes, the wind anomalies applied will be steady. The observational results of McPhaden and Zhang (2002) and Wielicki et al. (2001) are discussed in terms of the results.

2. An estimate of ocean heat transport

First, we present an idealized model of the wind-driven heat transport by the vertical and horizontal circulation. The heat transport by the meridional circulation is estimated with an idealized model of the subtropical cells that uses the observed wind stress and SST distributions [see the appendix; the model is essentially the same as that presented by Klinger and Marotzke (2000) and used by Held (2001)]. The model shows a distribution of heat transport that is qualitatively similar to observations. The maximum in the heat transport is at low latitudes. However, the maximum amplitude is only 0.53 PW at 7°N (see Fig. 1). The difference between the heat transport obtained from the simple model and the estimates derived from the atmospheric reanalysis data shows that heat transport by the wind-driven overturning circulation can only partly explain the total oceanic heat transport. A crude estimate of the amplitude of the heat transport carried by the horizontal gyres is made by determining the strength of the Sverdrup transport and the zonal asymmetry in temperature. It shows that the heat transport by the horizontal flow is not negligible. It acts to oppose the heat transport by the subtropical cells. The equatorward heat transport by the gyres in the Tropics is a consequence of the horizontal circulation bringing warm water toward the equator in the west and transporting relative cooler water poleward in the east.

As stated in the introduction a large contribution of the horizontal gyres to the heat transport has important consequences for how the Pacific ocean heat transport varies as climate varies. In the following we study the sensitivity of ocean heat transport in a model that ac-

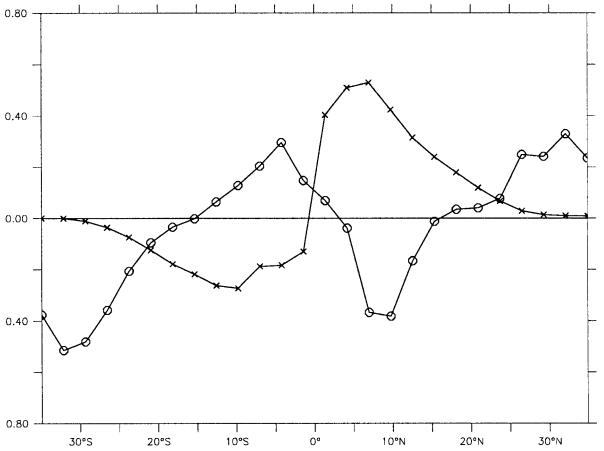

FIG. 1. Heat transport estimates in the Pacific Ocean (PW = 10^{15} W) derived from the simple models outlined in the appendix. Continuous with cross symbols: from idealized model of the wind-driven overturning using winds from the NCEP reanalysis data (Kalnay et al. 1996) and sea surface temperatures from the model introduced in section 2. Continuous with circles: from idealized model of gyre heat transport using NCEP reanalysis winds and temperatures from the model.

counts for the dominant mechanisms of ocean heat transport. The model and experiments are discussed in the following section.

3. Numerical model and experimental setup

a. Model

The experiments are performed with a primitive equation ocean model (Visbeck et al. 1998; Seager et al. 2001; Hazeleger et al. 2001a,b). The model has a resolution of 2.5° by 2.5° in the midlatitudes. The resolution in the meridional direction increases toward 0.5° at the equator. The model has 28 levels in the vertical. The model domain spans from 62°N to 62°S and from 90°E to 70°W. In the control experiment the ITF transport is set at 10 Sv (Sv $\equiv 10^6$ m^3 s^{-1}) and the Bering Strait is closed. The model contains a Krauss–Turner bulk mixed layer formulation and a one and a half layer thermodynamic ice model. An isopycnal thickness mixing scheme is incorporated. The vertical mixing has a background viscosity of 10^{-4} m^2 s^{-1} and a background tracer diffusion of 10^{-5} m^2 s^{-1}. The vertical mixing depends on the Richardson number. All side boundaries are closed and temperatures and salinities are restored to observations (Levitus and Boyer 1994; Levitus et al. 1994) when the model boundaries are ocean points. Also sea surface salinity is restored to observations (Levitus et al. 1994).

The ocean model is coupled to an atmospheric mixed-layer model (Seager et al. 1995) to create the so called Lamont Ocean–Atmospheric Mixed Layer Model (LOAM). The potential temperature and the humidity in the atmospheric mixed layer are computed from a balance between advection, surface fluxes, fluxes at the top of the mixed layer, and radiative fluxes. In addition, cooling by extratropical storms is parameterized (Hazeleger et al. 2001a). The wind speed and the wind stress are prescribed as well as air temperature and humidity over the land points [National Centers for Environmental Prediction (NCEP) reanalysis; Kalnay et al. (1996)]. Also the fractional cloudiness and solar radiation are prescribed [International Satellite Cloud Climatology Project; Bishop and Rossow (1991)]. The surface sensible and latent heat fluxes and the net surface radiation are internally computed in the model such that the SST is not overly constrained.

TABLE 1. Experiments.

Expt	Pattern	ITF transport (Sv)
Control	—	10
NINO	Fig. 2a	10
NINA	Fig. 2a (opposite sign)	10
NINO-ITF5	Fig. 2a	5
NINA-ITF15	Fig. 2a (opposite sign)	15
SPD1	Fig. 2b	10
SPD2	Fig. 2b (opposite sign)	10
SPEED	10% increase wind speed with respect to Control	10
STRESS	10% increase wind stress with respect to Control	10

The model has been spun up for 80 yr with the forcing as described above. The upper ocean is in equilibrium with the applied forcing. We refer to Hazeleger et al. (2001a) for more details on the model and a description of the climatology.

This model computes its own surface fluxes of latent and sensible heat and longwave radiation. The model is less constrained than in nature in that there is no equivalent of the globally averaged zero net radiative flux requirement at the top of the atmosphere. Nevertheless, it needs to be remembered that the tropical ocean heat transport varies mostly as a result of mechanical forcing of the ocean circulation and diapycnal mixing. The changes in mechanical forcing that we apply are realistic and the changes in ocean heat transport will also be realistic unless there are major changes in solar radiation, cloud cover, or ITF heat transport. The experiments will provide an estimate of by how much, and by what mechanisms, the ocean heat transport varies during low-frequency climate variations and provide suggestions for how the atmospheric heat transport or top of the atmosphere radiation will need to adjust.

b. Experiments

We investigate the response of the ocean heat transport in the model to changes in the atmospheric forcing (see Table 1). The dominant mode of climate variability in the Pacific is the El Niño–Southern Oscillation. It is most energetic at interannual time scales, but on decadal time scales ENSO-like variability occurs as well (Zhang et al. 1997). Therefore, to study the response of ocean

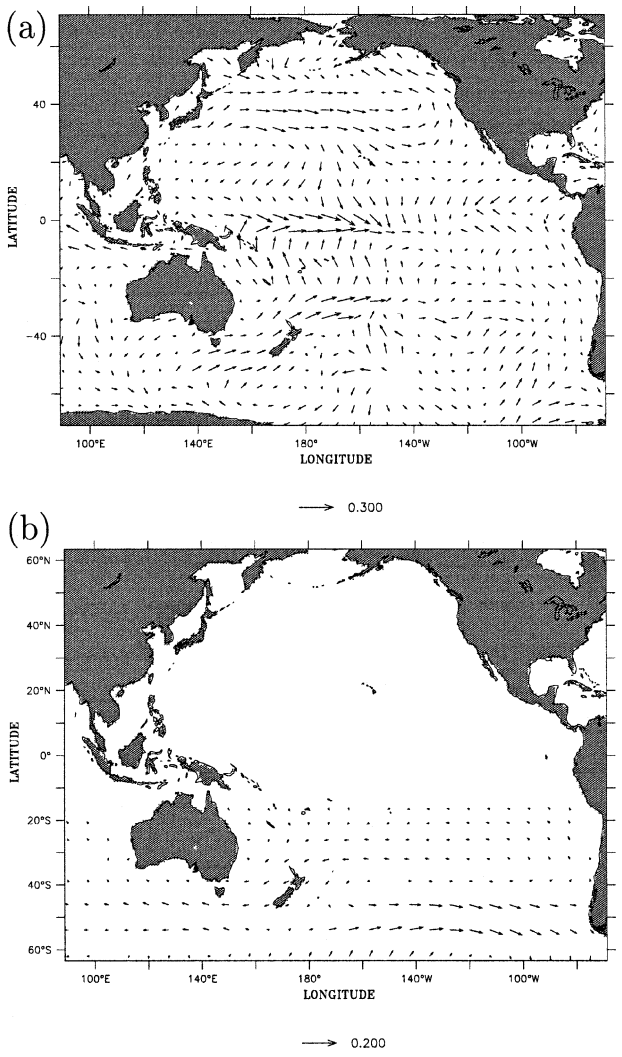

FIG. 2. (a) Anomalous El Niño–like wind stress pattern (N m^{-2}) used for experiments with tropical forcing anomalies (NINO, NINO-ITF5, and same pattern with opposite sign for NINA and NINA-ITF15; see Table 1). (b) Anomalous wind stress pattern used for experiments with South Pacific forcing anomalies (SPD).

heat transport to atmospheric variability in the Pacific it is natural to use the atmospheric part of the ENSO pattern as anomalous forcing. We obtained this pattern by regression of the wind stress, surface winds, and wind speed on the annual surface temperature anomaly in the NINO-3 box (5°N–5°S, 150°–90°W) [the wind stress pattern is shown in Fig. 2a; data from Da Silva et al. (1994)]. The wind pattern consists of a relaxing of the trade winds in an El Niño case (experiment NINO) and an increase in a La Niña case (experiment NINA). This pattern differs slightly from the pattern of decadal wind variations in the tropical Pacific. However, in this study we investigate the sensitivity of ocean heat transport to steady variations in atmospheric forcing and do not explicitly intend to simulate observed decadal variations. On the other hand, the main conclusions are not dependent on details of the wind pattern and will hold for decadal ENSO-like variability.

It has been observed that the strength of the ITF varies with the phase of the ENSO cycle. During an El Niño the trade winds relax and less water is transported through the ITF. The opposite occurs during a La Niña (Meyers 1996; Fieux et al. 1996; Vranes et al. 2002). In our model, the ITF is prescribed. To study the sensitivity of heat transport to its strength, we performed an experiment with a weak ITF (5 Sv) and El Niño–like wind anomalies (NINO-ITF5) and an experiment with a strong ITF (15 Sv) and La Niña–like wind anomalies (NINA-ITF15). Note that in the present model surface heat fluxes are internally computed and free to adjust, in contrast to the experiment with the completely closed ITF presented by Hirst and Godfrey (1993). However, the model does not capture dynamical coupled feedbacks such as those described by Schneider (1998).

The interaction of water masses between the extratropics and Tropics may also impact the heat transport at low latitudes. Once subducted in the extratropics water masses transfer to the Tropics while their properties hardly change in the nearly adiabatic interior of the ocean. On decadal time scales the impact of subduction of thermal anomalies from the extratropics on tropical variability is small, but on longer time scales it has been shown that the Tropics can respond to extratropical variability (Hazeleger et al. 2001a,b). In order to study the sensitivity of ocean heat transport to extratropical forcing anomalies we applied an anomalous wind pattern in the midlatitudes of the Southern Hemisphere (expts SPD1 and SPD2). This wind pattern is obtained by a regression of wind stress and wind speed on the time series of the first empirical orthogonal function of annual anomalies of SST in the South Pacific (south of 20°S). The winds have been tapered to zero around 20°S. This anomalous forcing consists mainly of an increase of the westerlies to the east of the date line between 40° and 50°S and a reduction of the westerlies to the west of the date line. The trades also enhance between 20° and 30°S to the east of 140°W (Fig. 2b).

In the model, the anomalous forcing acts through the momentum flux at the sea surface and wind speed and direction that effect the surface heat fluxes. To address both components separately we performed one run with increasing wind stresses (expt STRESS) and a run with increasing wind speed (expt SPEED).

The experiments have been run for 20 yr with the perpetual anomalous forcing. The tropical circulation is well adjusted within the 20 yr. The adjustment to extratropical forcing takes longer and those experiments have been run for 40 yr. We use data from the last year of the simulations.

4. Results

a. Climatological ocean heat transport

Figure 3 shows the meridional ocean heat transport in the Indo–Pacific Ocean in the control experiment. The meridional heat transport is equal to

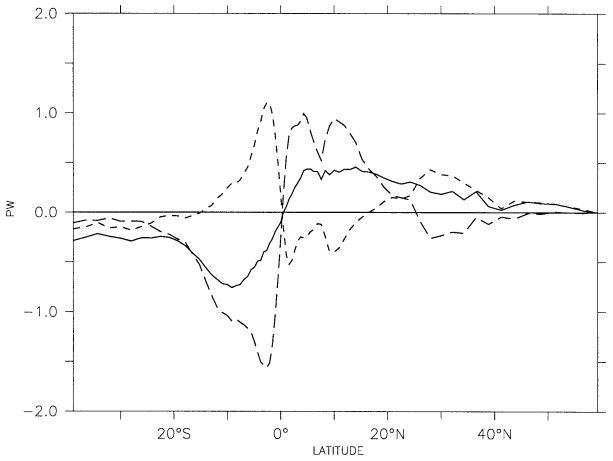

FIG. 3. Heat transport in the Indo–Pacific Ocean (PW = 10^{15} W) in the Control experiment. Continuous line: total transport; long dashes: overturning heat transport (OHT_{ovt}); short dashes: gyre heat transport (OHT_{gyre}).

$$\mathrm{OHT} = \rho_w c_p \int_H^0 \int_E^W vT \, dx \, dz, \tag{1}$$

where ρ_w is the density of seawater, c_p is the specific heat, v the meridional velocity, and T is the potential temperature. The temperature fluxes are integrated from top (0) to bottom (H) and from east (E) to west (W) to obtain heat transports. Note that mass flux through the boundaries must be zero for the heat transport to be invariant. In some cases we will mask out the Indian Ocean. In that case the temperature will be referenced to the basin-mean temperature.

To identify different physical mechanisms of meridional heat transport, the heat transport has been decomposed into three components (e.g., Bryan 1982):

$$\rho_w c_p[\overline{vT}] = \rho_w c_p[\overline{v}][\overline{T}] + \rho_w c_p[\overline{v^*}\,\overline{T^*}] + \rho_w c_p[\overline{v'T'}]. \tag{2}$$

Here the brackets denote the zonal integral, the asterisks denote deviations from the zonal mean, the primes denote deviation from the time mean, and the bars denote the time average. All terms are vertically integrated. In general, the last term is small in our model and we will neglect it from now on. We follow the usual conventions to call the first term on the right-hand side the overturning component heat transport (OHT_{ovt}) and the second term the gyre component of the heat transport (OHT_{gyre}).

The total heat transport has a peak close to the equator at a value of 0.45 PW at 5°N and −0.75 PW at 9°S. These values are lower than found by Trenberth and Caron (2001), but they are within error bars of observational estimates (Ganachaud and Wunsch 2003) and they are consistent with other model simulations (e.g., Semtner and Chervin 1992).

Figure 3 also shows OHT_{ovt} and OHT_{gyre}. Particularly

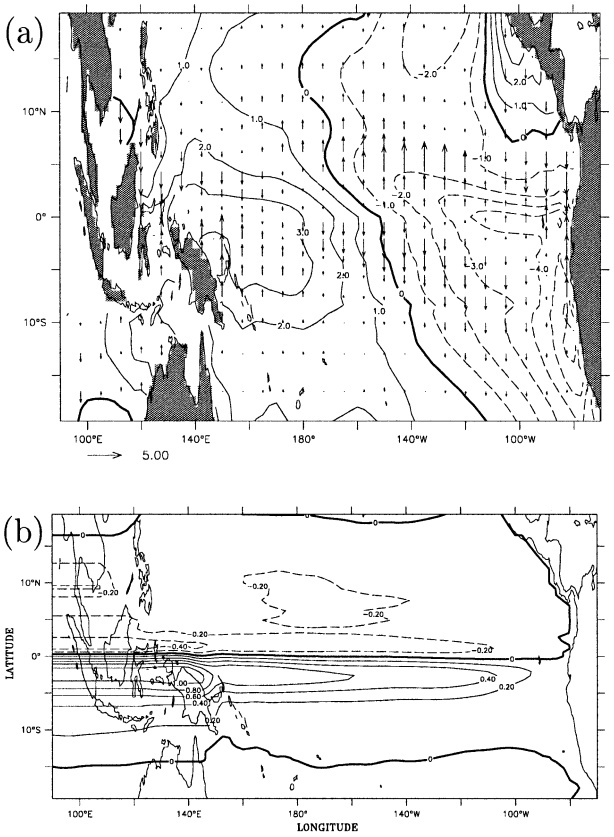

FIG. 4. (a) Deviation from the zonal mean surface temperature (contours, °C) and surface layer meridional velocity (vectors, 10^{-1} m s^{-1}) in expt Control (see Table 1). The upper layer in the model has a thickness of 10 m. (b) Indefinite integral of the OHT_{gyre} (PW), i.e., the vertically integrated temperature transport integrated from east to west in expt Control. The values on the western boundary correspond to the OHT_{gyre} in Fig. 3.

in the Tropics the individual components of the heat transport are larger than the total heat transport. The signs of both components can be easily understood from the mean circulation. The mean meridional overturning consists mainly of a subtropical cell that transports warm water at the surface away from the equator by Ekman divergence (e.g., Fig. 12a in Hazeleger et al. 2001a). When the water arrives in the subtropics, it has cooled and it subducts, driven by downward Ekman pumping and lateral flow through the sloping mixed layer. The subsurface adiabatic flow transfers the cooled water towards the equator where it upwells again to close the overturning circulation. This overturning is the main agent for the poleward OHT_{ovt}.

Most of the heat transport by the horizontal flow takes place in the upper thermocline. In order to understand the equatorward OHT_{gyre} in the Tropics we show the deviation from the zonal velocity and temperature in the upper 10 m (Fig. 4a). The temperature distribution shows the warm pool in the western Tropics and the cold tongue in the east stretching along the South American coast. The meridional flow is strongly poleward in

the center and eastern side of the basin caused by Ekman divergence. This flow carries water to the poles that is relatively cold compared to its zonal mean temperature, hence equatorward heat transport. When averaging the deviation of the zonally averaged meridional velocities over depth the effect of the boundary currents dominates (not shown). On the western side they are strongly equatorward. Due to the presence of the warm pool on the western side of the basin, this also implies equatorward heat transport. This is illustrated in Fig. 4b where we show the east to west indefinite integral of the gyre transport. The heat transport by the horizontal flow is equatorward over the entire zonal extension of the basin. The effect of the boundary currents on the heat transport is visible near 140°E where the integrated heat transport increases strongly toward the west.

The finding that the OHT_{gyre} is large in the Tropics is not new [for instance, Gordon et al. (2000), their Fig. 17], but it is important when interpreting causes of tropical SST changes on decadal time scales. Changes in heat transport by the horizontal gyres might be just as important as changes in the strength of the subtropical cells. Furthermore, it sheds light on the question of partitioning between atmospheric and oceanic heat transport under changing forcing. The simple model of a subtropical cell accounting for almost all the heat transport is not correct for the Pacific Ocean. Consistent with the crude estimate made in section 1, the heat transport by the horizontal gyre circulation appears to be just as important. So, the heat transports in the ocean and atmosphere need not increase and decrease together, which means that the response of the partitioning to changing forcing is not a priori clear.

b. Heat transport during perpetual El Niño and La Niña

The SST response to El Niño–like winds (expt NINO vs expt NINA) consists of a strong warming in the central Pacific and a cooling in the western and eastern tropical Pacific and a cooling at midlatitudes (see Fig. 5a). The SST anomalies in the model are a stationary response to changing winds. The response differs from the transient response, which is characterized by a strong warming in the cold tongue in the case of an El Niño. In the transient case, the response is dominated by planetery wave dynamics and transient deepening of the thermocline in the east causes warming. In the steady response, after adjustment of the circulation, the exact distribution of the anomalies in the Tropics appears to be forced by the local wind stress anomalies. The wind anomalies used (Fig. 2a) have strong westerlies in the center of the basin, which cause warming, and easterlies in the east, which cause cooling. The surface heat fluxes damp the temperature anomalies on the equator.

The differences between OHT in experiment NINO and NINA are shown in Fig. 6. As can be expected, large changes in the circulation occur as reflected in

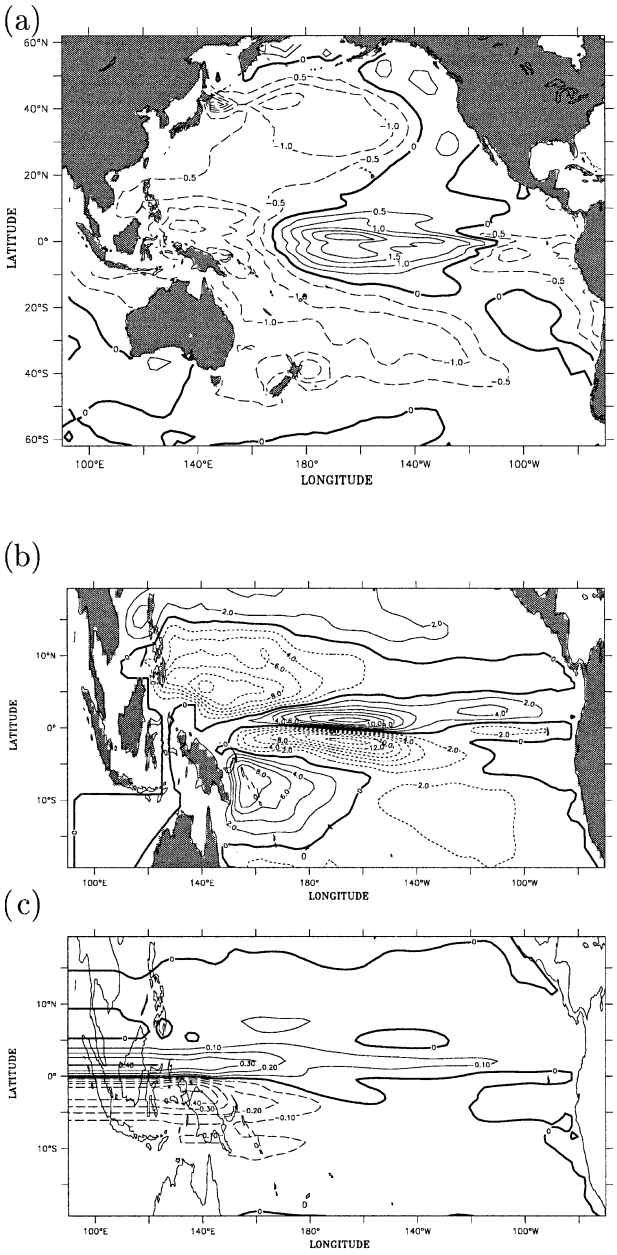

FIG. 5. (a) Difference between SST (°C) in expts NINO and NINA, (b) difference between barotropic streamfunction (Sv) in expts NINO and NINA, (c) difference between indefinite integral of OHT_{gyre} (PW) in expts NINO and NINA.

changes in OHT_{ovt} and OHT_{gyre}. However, strikingly, the changes nearly compensate to give a relatively small effect in the total heat transport. The heat transport is reduced by about 0.1 PW in the NINO case in comparison with the NINA case. This is still 20% of the total heat transport with changes in OHT_{ovt} exceeding changes in OHT_{gyre}. The strength of the cancellation of OHT_{gyre} and OHT_{ovt} may be fortuitous, but the sign of the opposing effect is robust and can be explained from the response of the wind-driven circulation to the anom-

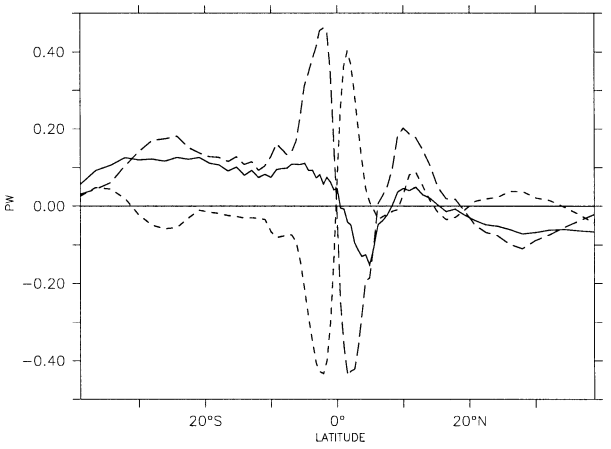

FIG. 6. Difference in ocean heat transport (PW = 10^{15} W) in the Indo–Pacific between expts NINO and NINA. Continuous line: difference in total heat transport; long dashed: difference in overturning heat transport (OHT_{ovt}); short dashed: difference in gyre heat transport (OHT_{gyre}).

alous winds. The meridional mean overturning circulation is weakened in the NINO case and enhanced in the NINA case. This is a direct response to the change in the zonal wind stress. In the NINO case reduced wind on the equator reduces the Ekman divergence and the associated upwelling. As a consequence the poleward heat transport by OHT_{ovt} is reduced by 0.4 PW in comparison with the NINA case.

The change in the horizontal circulation is visualized by the change in the barotropic streamfunction (Fig. 5b). Consistent with a reduction in the wind stress curl, the equatorial gyres spin down in the NINO experiment. The response is especially strong in the center of the basin where the largest wind anomalies occur. The change in the Sverdrup interior must be balanced by changes in the western boundary currents. Here the strongest changes in OHT_{gyre} occur (Fig. 5c). In the NINO case, the western boundary current transports strongly reduce and less heat is transported toward the equator. The changes in OHT_{gyre} in the interior are small.

Because both the strength of the gyre circulation and of the overturning circulation depend mainly on the zonal wind stress, a certain degree of compensation will always take place in response to changing zonal winds. To demonstrate that the response is dominated by the response to changes in wind stress, we show the anomalous heat transports in an experiment where only the wind speed has been increased by 10% over the entire basin (which effects the surface heat fluxes but leaves the circulation almost unchanged) and an experiment where the wind stress has been increased by 10% over the entire basin (which increases the ocean circulation while the surface fluxes simply respond; see Fig. 7). The change in the wind speed does not result in an increase of the OHT. It produces a zonally and vertically uniform temperature change (up to thermocline depth) that does not affect the heat transports. Changes in the wind stress, however, do change the heat transports. Heat transports by both the OHT_{ovt} and OHT_{gyre} increase as the gyres and the meridional mean overturning strengthen. The cancellation is strong but, as in the NINO and NINA cases, changes in the OHT_{ovt} exceed those in OHT_{gyre}, so the total heat transport increases by 0.1 PW, which is a 20% change for a 10% increase in wind stress. A linear relation between changes in wind stress and ocean heat transport is not warranted since a large part of the heat transport goes through the western boundary currents, which are of nonlinear nature. Also, the changes in the curl of the wind stress are expected to be just as important as the change in the gyre heat transport is as large as the change in the overturning heat transport.

A further analysis showed that the response of ocean heat transport to tropical wind anomalies is determined by anomalous mass transport acting on the mean tem-

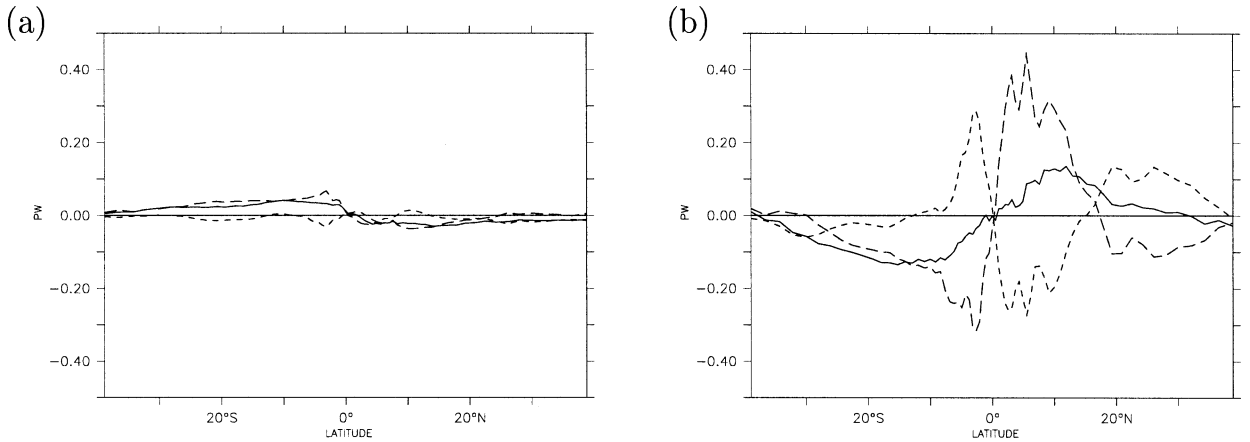

FIG. 7. Heat transports. (a) Difference between run with enhanced wind speed and control run (SPEED minus Control) and (b) difference between run with enhanced wind stress and control run (STRESS minus Control). Continuous line: total transport; long dashed: overturning heat transport (OHT_{ovt}); short dashed: gyre heat transport (OHT_{gyre}).

perature field, rather than the mean circulation working on anomalies in the temperature field. The compensation is brought about by changes in the wind-driven circulation as explained above.

c. Impact of varying ITF on the heat transport

As mentioned before, a change in the zonal winds in the Tropics affects the volume transport through the ITF from the Pacific toward the Indian Ocean. When the trade winds relax, the volume transport decreases. Two experiments are performed to study the effect of varying ITF volume transport on the heat transport in the Pacific. In the first case we applied the El Niño–like anomalous winds and fixed the volume transport in the ITF to 5 Sv, instead of 10 Sv as in the previous section. In the second case we applied winds of the opposite sign and increased the ITF to 15 Sv.

The differences between heat transports in experiments with an ITF of 10 Sv (NINA) and an ITF of 15 Sv (NINA-ITF15) are shown in Figs. 8a and 8b. The heat transports in the Southern Hemisphere respond most strongly to the change in ITF transport, with stronger poleward heat transport when the ITF volume transport is larger. More warm water is transported from the tropical Pacific Ocean into the Indian Ocean, which warms (see Fig. 9). The South Pacific cools, especially in the East Australia Current, but also in the cold tongue in the tropics. In the Pacific alone, increased ITF causes increased northward heat transport in the Southern Hemisphere, while the divergence of the ocean heat transport, as determined by the difference in heat transport in the ITF and at 30°S causes the Pacific basin to cool when the ITF is stronger (see Table 2).

This response is consistent with the complete closing experiments of Hirst and Godfrey (1993) and Schneider (1998). However, note that our model does not include a complete Indian Ocean and that the response in the Agulhas region is not simulated; hence the amplitude of the response may be unrealistic. Too much heat might

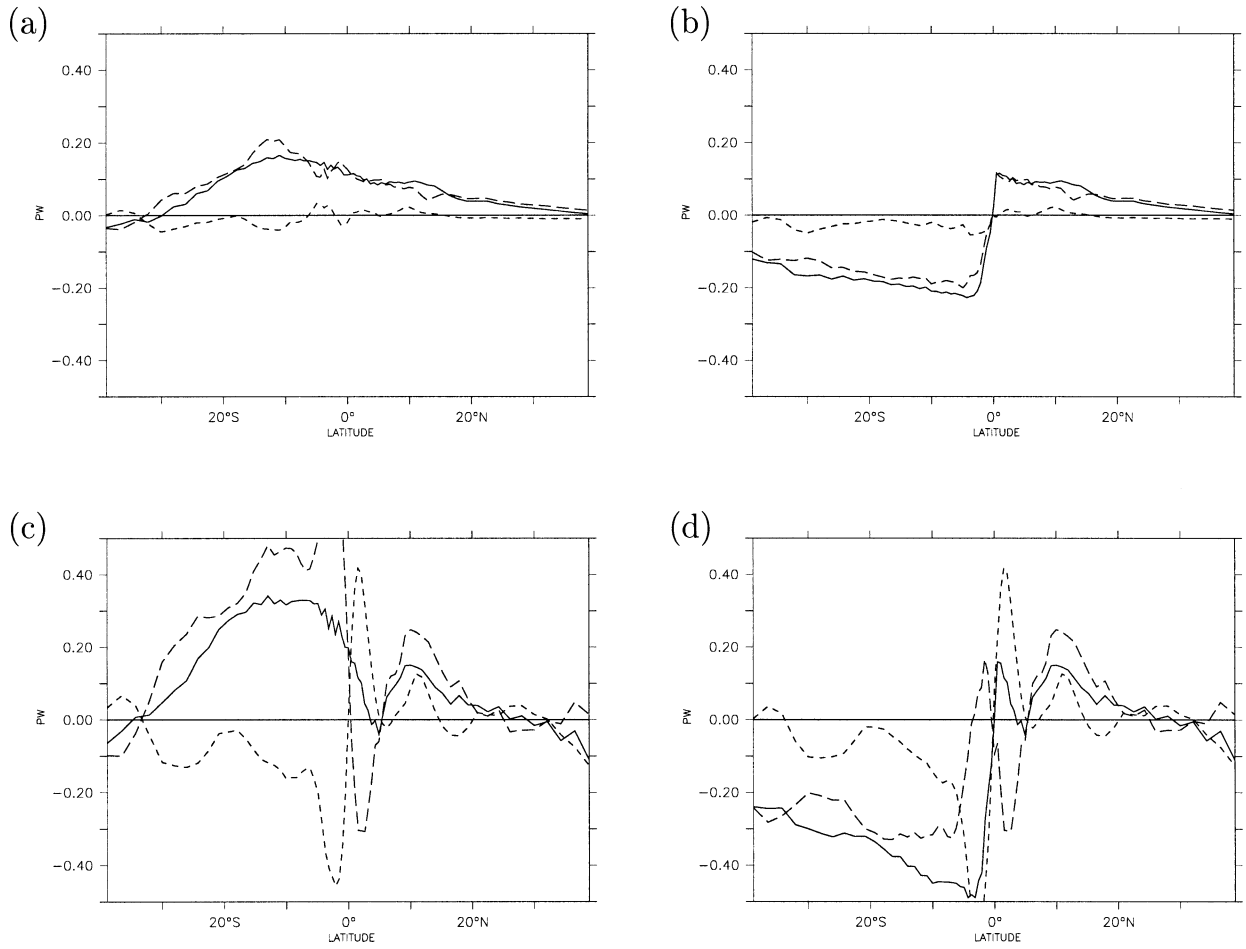

FIG. 8. Heat transports. (a) Difference between ITF 10 Sv and ITF 15 Sv (NINA minus NINA-ITF15) and (b) as in (a) but without Indian Ocean (NINA minus NINA-ITF15); (c) difference between ITF 5 Sv and El Niño winds and ITF 15 Sv and La Niña winds (NINO-ITF5 minus NINA-ITF15) and (d) as in (c) but without Indian Ocean. Continuous line: total transport; long dashed: overturning heat transport (OHT_{ovt}); short dashed: gyre heat transport (OHT_{gyre}).

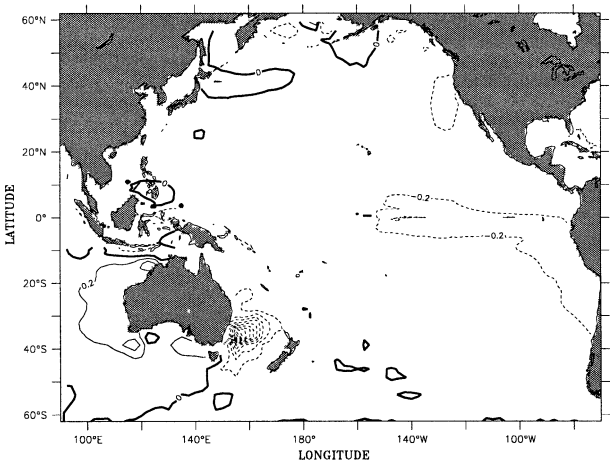

FIG. 9. Difference between SST (°C) in expt NINA-ITF15 and expt NINA, i.e., the effect of enhanced ITF transport on SST.

transfer back into the South Pacific without being vented off to the atmosphere. The change in the OHT is completely determined by a change in the OHT_{ovt}. A complete closure as in Hirst and Godfrey (1993) almost certainly also affects the OHT_{gyre} significantly.

When changes in the winds are combined with changes in the ITF volume transport, the almost exact cancellation of OHT_{gyre} and OHT_{ovt} breaks down. The heat transport in the Northern Hemisphere is hardly affected by changes in the ITF, but the Southern Hemisphere heat transports respond strongly (Figs. 8c,d). The response of OHT_{gyre} is very similar to that in experiments NINO and NINA; it is the OHT_{ovt} that responds differently. The changes in heat transport due to tropical wind variability and variability in ITF transport are almost linearly additive.

d. Response to extratropical anomalous wind forcing

Last, we study how anomalous atmospheric forcing in the extratropics can affect tropical ocean heat transport. In the midlatitudes water subducts and flows subsurface toward the equator where it upwells again. Anomalous atmospheric forcing in the extratropics can potentially influence the tropical stratification. Model studies indicate that this mechanism does not produce anomalies of significant amplitude on decadal time scales (Schneider et al. 1999; Hazeleger et al. 2001b). However, on longer time scales the tropical thermocline can be influenced by the extratropical forcing anomalies. Hazeleger et al. (2001a) found that cooling of about 40 W m^{-2} by transient eddy fluxes in the atmosphere in the extratropics can cool the tropical thermocline by as much as 1 K.

Here we applied a typical atmospheric forcing anomaly to the model in the South Pacific (Fig. 2b). The response of the OHT is an increase in poleward heat transport in the Southern Hemisphere in experiment

TABLE 2. Heat transports (PW) at sections at the ITF latitude and at 30°S in the Pacific only.

Expt	ITF	Pacific 30°S
Control	−0.92	0.25
NINO	−0.88	0.27
NINA	−0.97	0.17
NINO-ITF5	−0.48	−0.04
NINA-ITF15	−1.4	0.4

SPD1 compared to experiment SPD2 (see Fig. 10). Strengthening of the westerlies in the southern midlatitudes east of the date line induces a cooling (see Fig. 11a). The westerlies decrease west of the date line and the SST warms. This is due to changes in surface heat loss induced by the wind variations. The subsurface response is rather different. The cooler waters in the eastern midlatitudes subduct and spread westward subsurface along 15°S (Fig. 11b). This cooling in the east sets up an anomalous overturning circulation that reaches into the Tropics and even into the North Pacific (Fig. 12). The changes in the total heat transport within the Tropics are as big as in the NINO/NINA experiments. The anomalous overturning does not consist of a change in the wind-driven subtropical cell. In this case, it is a deeper reaching buoyancy-driven overturning circulation. Its downwelling branch is located at the region of maximal cooling, which is much farther south than the downwelling branch of the subtropical cell that is related to Ekman pumping. The strength of this anomalous overturning is proportional to the meridional density gradient and the vertical diffusivity in the interior of the ocean (e.g., Gnanadesikan 1999). The anomalous warm waters in the western midlatitudes spreads out subsurface to the east. The warming in the midlatitudes and cooling in the subtropics is consistent with the convergence of ocean heat transport poleward of 30°S and divergence equatorward of 30°S.

The lack of a contribution of OHT_{gyre} is due to the

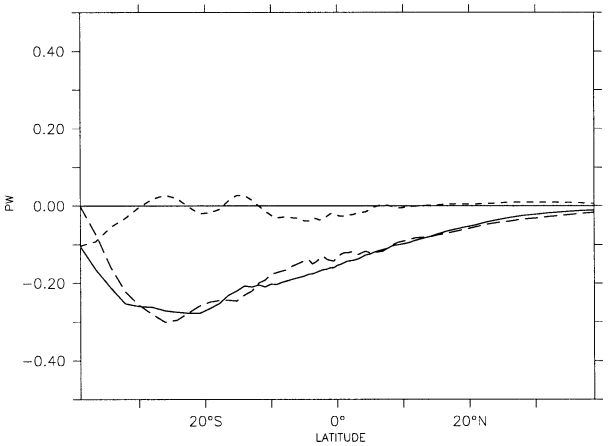

FIG. 10. Difference in heat transport in SPD1 and SPD2 (PW = 10^{15} W). Continuous line: total transport; long dashed: overturning heat transport (OHT_{ovt}); short dashed: gyre heat transport (OHT_{gyre}).

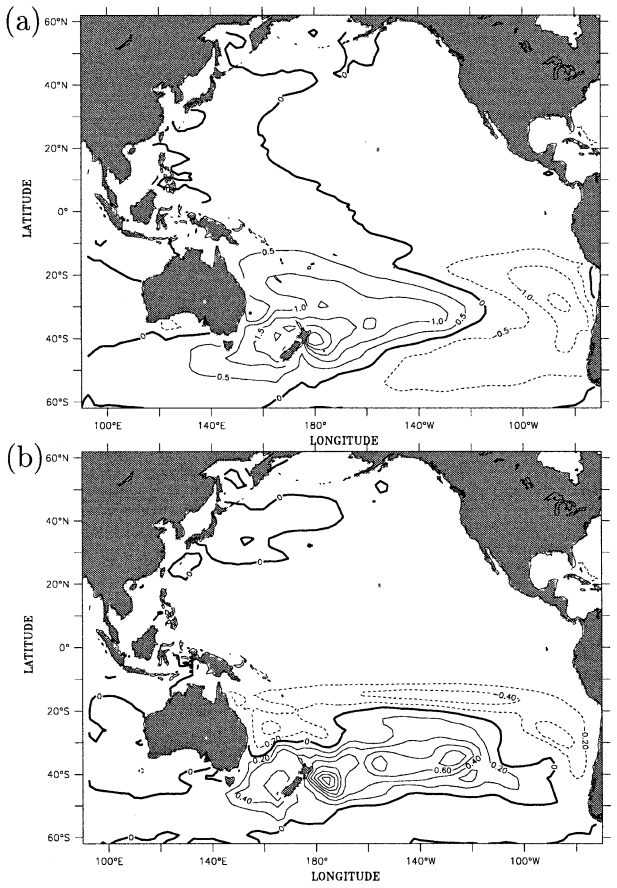

FIG. 11. (a) Difference between SST (°C) in expts SPD1 and SPD2 and (b) difference between temperature averaged over the top 1000 m (°C) in expts SPD1 and SPD2.

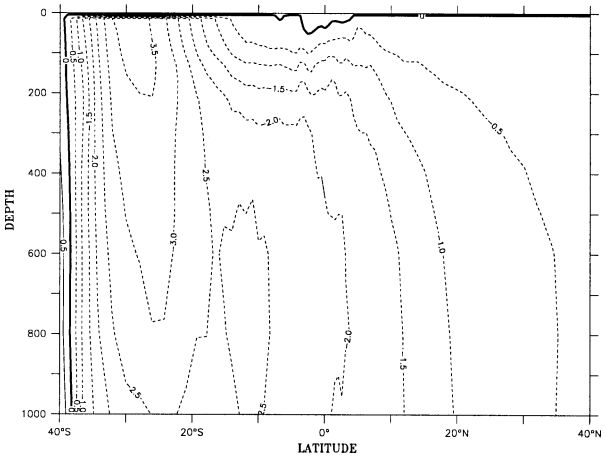

FIG. 12. Difference in meridional overturning in SPD1 and SPD2 (Sv).

small zonal deviations in the temperature anomalies that are generated. While the SST cools in the east and warms in the west, the vertically integrated temperature has hardly any zonal variation (Fig. 11b). The horizontal barotropic transport is enhanced with 18 Sv, but due to the small temperature variations this hardly affects OHT_{gyre}.

When analyzing whether the anomalous heat transport is caused by changes in mean mass transports or changes the temperature field, it appeared that anomalies in the mass transport are important for anomalies in heat transport in the extratropics. The anomalous heat transport in the Tropics is mainly determined by anomalies in the subsurface temperature field, which are transferred to the tropics by the meridional overturning circulation. A similar result was found by Hazeleger et al. (2001a, their Figs. 12 and 13).

The influence of the midlatitudes on the Tropics complicates the idealized picture of heat transport by coupled overturning circulations in the atmosphere and ocean. Tropical heat transport is driven by a buoyancy-driven overturning cell that extends into the midlatitudes, as well as by a low-latitude wind-driven overturning. Since the buoyancy-driven influences do not change tropical SST (see Fig. 12), presumably the tropical atmospheric circulation—including heat transport—is unchanged.

5. Discussion and conclusions

The mechanisms and sensitivity of heat transport in the tropical Pacific have been investigated in this paper. Here, we have shown that the gyre transport moves almost as much heat equatorward as the Ekman overturning moves poleward. Further, we have shown that the wind-driven mean meridional overturning only accounts for half of the total overturning transport in the model. The remainder must be buoyancy-driven, partly due to strong mixing near the equator. The results imply that the heat transport and the partitioning between atmospheric and oceanic heat transport may be more variable than suggested by Held (2001). This study also has implications for causes of the observed decadal SST variations in the tropical Pacific as explained below in section 5b.

a. Summary of model results

By applying El Niño–like wind anomalies, we studied the effect of long term El Niño–like variability on the heat transport. We study the stationary response of ocean heat transport to atmospheric forcing. The response of the model bears resemblance to decadal variations found in observations. The SST response consists of a strong warming in the center of the tropical Pacific, hardly any change in the cold tongue, and cooling in the midlatitudes. The pattern differs from the transient response of the ocean during the interannual El Niño cycle. In that case, the cold tongue is strongly affected. Zhang et al. (1997) did find cold tongue transitions at low frequencies, but the response in the cold tongue depends on the particular time analyzed.

The response of the heat transport to the large El Niño–like changes is relatively small, but significant (0.05 PW, a 10% change compared to the Control experiment). Large changes in the circulation occur that impact the overturning and the gyre circulations. The El Niño–like winds imply relaxing of the trades and reduced Ekman-driven overturning transport, hence reduced overturning heat transport by as much as 0.2 PW. However, the Sverdrup response of the gyres implies a slow down of the horizontal circulation. This causes equatorward heat transport by the horizontal flow to reduce, thereby compensating the reduction in poleward overturning heat transport. In our model the changes in the overturning heat transport are larger, such that persistent El Niño–like forcing induces a reduction in poleward heat transport. These changes are brought about by wind-driven changes in the circulation rather than the change in stratification.

The tropical Pacific is not a closed system, and the picture gets complicated by transport of heat to other regions. The ITF transports large amounts of heat into the Indian Ocean consistent with earlier model studies. Our results showed that reduced ITF transport, as observed during ENSO, cools the Indian Ocean and warms the South Pacific Ocean. The ocean heat transport only responds in the Southern Hemisphere. Increased ITF transport increases the poleward heat transport in the Indian Ocean and decreases it in the South Pacific (0.2-PW reduction), which therefore cools. In the equatorial Pacific the reduced ITF and El Niño–like winds cause the poleward heat transport to decrease by about 0.1 PW.

Extratropics–Tropics interaction can also influence tropical ocean heat transport in our model. Changes in extratropical atmospheric circulation can excite a buoyancy-driven overturning that reaches into the Tropics, but leaves tropical SST unchanged. Cooling in the extratropics increases the poleward oceanic heat transport by 0.1 PW in the Tropics.

In conclusion, tropical ocean heat transport is less sensitive to tropical atmospheric variability than expected from wind-driven changes in the meridional overturning cells alone and the impact of the gyres cannot be neglected. Also, changes in the ITF and buoyancy forcing in the extratropics have a large impact on tropical ocean heat transport. Increased ITF transport will reduce poleward heat transport in the South Pacific, while cooling in the midlatitudes tends to enhance poleward heat transport in the Tropics. These findings were obtained in a model that ignores the dynamical response of the atmosphere to variations in ocean heat transport. Nevertheless, it is clear that the idealized model for meridional heat transport in the tropics as envisaged by Held (2001) is invalid. Note, however, that the theory of Held (2001) may more properly apply to the zonal mean over the globe while we study only the Pacific here. However, in our model the heat transport cannot simply be explained by a tight coupling between the atmosphere and ocean mean meridional overturning heat transport. An important conclusion is that the oceanic heat transports are not tightly constrained to the atmospheric heat transport due to the large heat transport by the horizontal gyre flow. The compensating effect of overturning and gyre heat transport in the Tropics is a robust effect that can be understood from the response of the wind-driven circulation to atmospheric variability. However, the picture gets complicated by external sources and sinks of heat, such as the ITF and heat transport to and from the midlatitudes.

b. Relation to observed decadal changes in the tropical Pacific

Observations show that the oceanic overturning mass transport has decreased steadily from the mid 1970s to the late 1990s (McPhaden and Zhang 2002). Over this period the SST in the equatorial Pacific has increased and the winds have become more akin to a typical El Niño pattern with weaker trade winds. McPhaden and Zhang do not rule out the impact of the gyres, but they suggest that decreased meridional overturning caused a reduction in poleward heat transport that caused the equatorial warming with the changes in SST being damped by surface fluxes. Nonaka et al. (2002) supported this by deriving a relation between meridional heat transport and tropical SSTs from an ocean model. Our results indicate that it is premature to deduce changes in the total ocean heat transport from changes in the overturning alone because we also expect that reduced trade winds would reduce the equatorward heat transport by the gyres and also reduce the ITF (although the latter would add to the changes in overturning heat transport in the South Pacific). An empirical relation between changes in overturning strength and decadal tropical SST variability, as found be Nonaka et al. (2002), may work as changes in overturning and gyre transport, and possibly ITF transport, act in concert in response to tropical wind stress changes. Since we find that wind-driven changes in the circulation acting on the mean temperature field determine the changes in ocean heat transport, a linear relation between overturning strength and SST changes can be found. However, the slope obtained from such a linear regression will probably be incorrect as changes in gyre heat transport are not taken into account. Also, such a relation is not expected to work for longer time scales. In that case, the impact of anomalous buoyancy forcing in the midlatitudes becomes important, and tropical ocean heat transport anomalies cannot be related to anomalous wind stress in the subtropics alone. The changes in total poleward ocean heat transport from the mid 1970s to the late 1990s is the sum of these different processes and is unknown.

The reduced ocean overturning from the mid 1980s to the late 1990s is consistent with reduced meridional overturning in the atmosphere over the Pacific Ocean

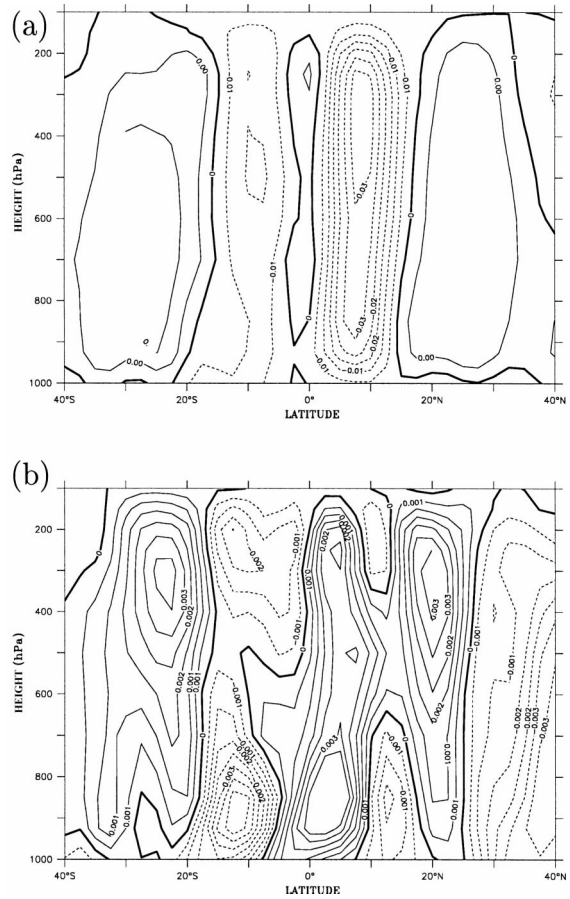

FIG. 13. (a) Zonal mean pressure vertical velocity (Pa s^{-1}) in the Pacific (130°E, 70°W) averaged from 1985 to 2000 as obtained from NCEP reanalysis data (Kalnay et al. 1996). (b) Difference between zonal mean pressure vertical velocity in the Pacific (1993–2000 minus 1985–92).

during the same time period (Fig. 13). However, a reduced Pacific sector Hadley cell need not mean reduced poleward heat transport in the atmosphere. The warming of the equatorial Pacific and the cooling in the subtropics causes the moist static energy gradient to change; hence advection of moist static energy by the mean overturning can compensate the reduced transport of mean moist static energy by the reduced overturning.

Wielicki et al. (2002) report that over the mid 1980s to late 1990s period the net incoming radiation at the top of the atmosphere over the tropics between 20°N and 20°S was reduced by about 4 W m^{-2}. The changes in ocean heat transport suggested by McPhaden and Zhang (2002), and the reduced Pacific sector Hadley cell shown in Fig. 13, only circulate heat within the Tropics. The net radiative loss in the Tropics indicated by Wielicki et al. needs to be balanced by either reduced heat export from the tropical atmosphere or ocean to higher latitudes or by reduced heat storage in the tropical ocean. A 4 W m^{-2} reduction in net incoming radiation over 20°S to 20°N requires a 0.5 PW reduction in the sum of the poleward heat transports across the northern and southern boundaries. Our results show that this represents a very large (about 50%) change in the ocean heat transport, and none of our experiments lead to changes in the heat transport by anywhere near that much. It is a much smaller fractional change of the atmospheric heat transport. The large tropical ocean warming over this time period makes reduction of ocean heat storage an unlikely balancing mechanism. More work is required to clarify the physical mechanisms that underlie such changes in the regional radiative balance of the climate system and apparent changes in partitioning of the total heat transport between the atmosphere and ocean.

Acknowledgments. Author WH thanks the people at LDEO for their hospitality during his stay. Martin Visbeck is thanked for discussions and suggestions on the topic. Comments of M. McPhaden and of the reviewers are appreciated. Authors RS, MAC, and NN were supported by NOAA Grants UCSIO PO 10196097 and NA16GP2024, and NSF Grant ATM-9986515.

APPENDIX

Idealized Models of Ocean Heat Transport

a. An idealized model of heat transport by the subtropical cells

The heat transport in the wind-driven subtropical cell can be estimated from the surface conditions only. We assume that the poleward upper branch of the subtropical cells is in the upper layer and the equatorward return flow in the interior. In this case, the ocean heat transport in the surface layer can be estimated using (all zonal integrals are omitted for clarity):

$$\mathrm{OHT}_s(y) = \rho_w c_p v_s(y) H T_s(y), \qquad \text{(A1)}$$

with ρ_w being the density of water, c_p the heat capacity of water, v_s the meridional surface velocity, H the thickness of the upper layer, and T_s the sea surface temperature, and y the latitude. For simplicity latitudinal and longitudal dependencies of x and y are omitted here.

The ocean heat transport in the return flow in the interior is equal to

$$\mathrm{OHT}_i(y) = \rho_w c_p \int_H^Z v_i(y) T_i(y)\, dz. \qquad \text{(A2)}$$

Using mass conservation and the assumption that diapycnal transports are zero in the interior [this approach is similar to Klinger and Marotzke (2000)], the equatorward meridional mass and heat transport at a section in the interior should balance the total mass and heat transport that is pumped down northward of the section:

$$\mathrm{OHT}_i(y) = \rho_w c_p \int_H^Z v_i(y) T_i(y)\, dz$$

$$= \rho_w c_p \int_{y_n}^{y} w(y') T_s(y')\, dy'. \qquad \text{(A3)}$$

From mass conservation $w(y') = -H\partial v_s(y')/\partial y$. Integrating by parts leads to the following relation for the total surface and interior ocean heat transport:

$$\mathrm{OHT}(y) = \rho_w c_p v_s(y_n) T(y_n) H - \rho_w c_p H \int_{y_n}^{y} v_s \frac{\partial T_s}{\partial y'}\, dy'. \qquad \text{(A4)}$$

Here y_n is the northern boundary of the subtropical cell. The surface velocity v_s can be derived from the Ekman transport. Here we will use a frictional Ekman balance, such that the transport near the equator can be included:

$$v_s = \frac{1}{\rho_w (f^2 + r^2)} (r\tau_y - f\tau_x), \qquad \text{(A5)}$$

with f being the Coriolis parameter, r a linear friction parameter (order of days), and τ_x and τ_y the zonal and meridional wind stress.

b. An idealized model of heat transport by the gyres

Using the Sverdrup balance an estimate can be obtained of the heat transport by the horizontal gyres. We assume that the transport in the western boundary currents compensate the transport in the interior (i.e., away from the western boundary currents), such that the heat transport by the gyres is

$$\mathrm{OHT}_{\mathrm{gyre}} = D\rho_w c_p \left(T_b \int_{x_w}^{x_{wb}} v_b\, dx + \int_{x_{wb}}^{x_e} v_{\mathrm{int}} T_{\mathrm{int}}\, dx \right). \qquad \text{(A6)}$$

Here D is the depth, T_b is the temperature in the western boundary current, T_{int} is the temperature away from the western boundary, x_e is the longitude of the eastern boundary, x_w is the longitude of the western boundary, and x_{wb} is the latitude of the eastern edge of the western boundary current. Using the Sverdrup balance, the heat transport by the gyres is (with $\beta = df/dy$)

$$\mathrm{OHT}_{\mathrm{gyre}} = \frac{c_p}{\beta} \frac{\partial \tau_x}{\partial y} (T_{\mathrm{int}} - T_b)(x_e - x_{wb}). \qquad \text{(A7)}$$

REFERENCES

Bishop, J. K. B., and W. B. Rossow, 1991: Spatial and temporal variability of global surface solar irradiance. *J. Geophys. Res.,* **96,** 16 839–16 858.

Bjerknes, J., 1964: Atlantic air/sea interaction. Advances in Geophysics, Vol. 10, Academic Press, 1–82.

Bryan, K., 1982: Seasonal variation in meridional overturning and poleward heat transport in the Atlantic and Pacific Oceans: A model study. *J. Mar. Res.,* **40** (Suppl.), 39–53.

Clement, A. C., and R. Seager, 1999: Climate and the tropical oceans. *J. Climate,* **12,** 3383–3401.

Cohen-Solal, E., and H. Le Treut, 1997: Role of the oceanic heat transport in climate dynamics: A sensitivity study with an atmospheric general circulation model. *Tellus,* **49A,** 371–387.

Covey, C., and S. L. Thompson, 1989: Testing effects of ocean heat transport on climate. *Palaeogeogr. Palaeoclim. Palaeoecol.,* **75,** 331–341.

Da Silva, A. M., C. C. Young, and S. Levitus, 1994: *Algorithms and Procedures.* Vol. 1, *Atlas of Surface Marine Data 1994,* NOAA Atlas NESDIS 6, 83 pp.

Fieux, M., R. Molcard, and A. G. Ilahude, 1996: Geostrophic transport of the Pacific–Indian Oceans Throughflow. *J. Geophys. Res.,* **101,** 12 421–12 432.

Ganachaud, A., and C. Wunsch, 2000: Improved estimates of global ocean circulation, heat transport and mixing from hydrographic data. *Nature,* **408,** 453–457.

——, and ——, 2003: Large-scale ocean heat and freshwater transports during the World Ocean Circulation Experiment. *J. Climate,* **16,** 696–705.

Gnanadesikan, A., 1999: A simple predictive model for the structure of the oceanic pycnocline. *Science,* **283,** 2077–2079.

Gordon, C., and Coauthors, 2000: The simulation of SST, sea ice extents and ocean heat transports in a version of the Hadley Centre coupled model without flux adjustments. *Climate Dyn.,* **16,** 147–168.

Guilderson, T. P., and D. P. Schrag, 1998: Abrupt shift in subsurface temperatures in the tropical Pacific associated with changes in El Niño. *Science,* **281,** 240–243.

Hazeleger, W., R. Seager, M. Visbeck, N. Naik, and K. Rodgers, 2001a: Impact of midlatitude storm track on the upper Pacific Ocean. *J. Phys. Oceanogr.,* **31,** 616–636.

——, M. Visbeck, M. Cane, A. Karspeck, and N. Naik, 2001b: Decadal upper ocean variability in the tropical Pacific. *J. Geophys. Res.,* **106,** 8971–8988.

Held, I. M., 2001: The partitioning of the poleward energy transport between the tropical ocean and atmosphere. *J. Atmos. Sci.,* **58,** 943–948.

Hirst, A. C., and J. S. Godfrey, 1993: The role of the Indonesian Throughflow in a global GCM. *J. Phys. Oceanogr.,* **23,** 1057–1086.

Jayne, S. R., and J. Marotzke, 2001: The dynamics of ocean heat transport variability. *Rev. Geophys.,* **39,** 385–411.

Kalnay, E., and Coauthors, 1996: The NCEP/NCAR 40-Year Reanalysis Project. *Bull. Amer. Meteor. Soc.,* **77,** 437–471.

Klinger, B. A., and J. Marotzke, 2000: Meridional heat transport by the Subtropical Cell. *J. Phys. Oceanogr.,* **30,** 696–705.

Levitus, S., and T. P. Boyer, 1994: *Temperature.* Vol. 4, *World Ocean Atlas 1994,* NOAA Atlas NESDIS 4, 117 pp.

——, R. Burgett, and T. P. Boyer, 1994: *Salinity.* Vol. 3, *World Ocean Atlas 1994,* NOAA Atlas NESDIS 3, 99 pp.

Liu, Z., 1994: A simple model of the mass exchange between the subtropical and tropical ocean. *J. Phys. Oceanogr.,* **24,** 1153–1165.

McCreary, J. P., and P. Lu, 1994: Interaction between the subtropical and tropical ocean. *J. Phys. Oceanogr.,* **24,** 1153–1165.

McPhaden, M. J., and D. Zhang, 2002: Slowdown of the meridional overturning circulation in the upper Pacific Ocean. *Nature,* **415,** 603–608.

Meyers, G., 1996: Variation of the Indonesian Throughflow and the El Niño–Southern Oscillation. *J. Geophys. Res.,* **101,** 12 255–12 263.

Nonaka, M., S. P. Xie, and J. P. McCreary, 2002: Decadal variations in the Subtropical Cells and equatorial SST. *Geophys. Res. Lett.,* **29,** doi:10.1029/2001GL013717.

Schneider, N., 1998: The Indonesian Throughflow and the global climate system. *J. Climate,* **11,** 676–689.

——, S. Venzke, A. J. Miller, D. W. Pierce, T. P. Barnett, C. Deser, and M. Latif, 1999: Pacific thermocline bridge revisited. *Geophys. Res. Lett.,* **26,** 1329–1332.

Seager, R., M. B. Blumenthal, and Y. Kushnir, 1995: An advective atmospheric mixed-layer model for ocean modeling purposes: Global simulation of surface heat fluxes. *J. Climate,* **8,** 1951–1964.

——, Y. Kushnir, N. H. Naik, M. A. Cane, and J. Miller, 2001: Wind-driven shifts in the latitude of the Kuroshio–Oyashio extension and generation of SST anomalies on decadal timescales. *J. Climate,* **14,** 4249–4265.

Semtner, A. J., and R. M. Chervin, 1992: Ocean general circulation from a global eddy resolving model. *J. Geophys. Res.,* **97,** 5493–5550.

Timmermann, A., M. Latif, A. Bacher, J. Oberhuber, and E. Roeckner, 1999: Increased El Niño frequency in a climate model forced by future greenhouse warming. *Nature,* **398,** 694–696.

Trenberth, K. E., and J. M. Caron, 2001: Estimates of meridional atmosphere and ocean heat transports. *J. Climate,* **14,** 3433–3443.

Visbeck, M., H. Cullen, G. Krahmann, and N. Naik, 1998: An ocean's model response to North Atlantic Oscillation-like wind forcing. *Geophys. Res. Lett.,* **25,** 4521–4524.

Vranes, K., A. L. Gordon, and A. Ffield, 2002: The heat transport of the Indonesian Throughflow and implications for the Indian Ocean heat budget. *Deep-Sea Res.,* **49B,** 1391–1410.

Wielicki, B. A., and Coauthors, 2002: Evidence for large decadal variability in the tropical mean radiative energy budget. *Science,* **295,** 841–844.

Zhang, Y., J. M. Wallace, and D. S. Battisti, 1997: ENSO-like interdecadal variability: 1900–1993. *J. Climate,* **10,** 1004–1020.